Long journey into tunneling*

Leo Esaki

IBM Thomas J. Watson Research Center, Yorktown Heights, New York 10598

I. HISTORICAL BACKGROUND

In 1923, during the infancy of the quantum theory, de Broglie (1923, 1925) introduced a new fundamental hypothesis that matter may be endowed with a dualistic nature—particles may also have the characteristics of waves. This hypothesis, in the hands of Schrödinger (1926) found expression in the definite form now known as the Schrödinger wave equation, whereby an electron or a particle is assumed to be represented by a solution to this equation. The continuous nonzero nature of such solutions, even in classically forbidden regions of negative kinetic energy, implies an ability to penetrate such forbidden regions and a probability of tunneling from one classically allowed region to another. The concept of tunneling, indeed, arises from this quantum-mechanical result. The subsequent experimental manifestation of this concept can be regarded as one of the early triumphs of the quantum theory.

In 1928, theoretical physicists believed that tunneling could occur by the distortion, lowering or thinning, of a potential barrier under an externally applied high electric field. Oppenheimer (1928) attributed the autoionization of excited states of atomic hydrogen to the tunnel effect: The Coulombic potential well which binds an atomic electron could be distorted 'by a strong electric field so that the electron would see a finite potential barrier through which it could tunnel.

Fowler and Nordheim (1928) explained, on the basis of electron tunneling, the main features of the phenomenon of electron emission from cold metals by high external electric fields, which had been unexplained since its observation by Lilienfeld in 1922. They proposed a one-dimensional model. Metal electrons are confined by a potential wall whose height is determined by the work function ϕ plus the Fermi energy E_f, and the wall thickness is substantially decreased with an externally applied high electric field, allowing electrons to tunnel through the potential wall, as shown in Fig. 1 They successfully derived the well known Fowler–Nordheim formula for the current as a function of electric field F:

$$J = AF^2 \exp[-4(2m)^{1/2}\phi^{3/2}/3\hbar F].$$

An application of these ideas, which followed almost immediately, came in the model for α decay as a tunneling process put forth by Gamow (1928) and Gurney and Condon (1928). Subsequently, Rice (1929) extended this theory to the description of molecular dissociation.

The next important development was an attempt to invoke tunneling in order to understand transport properties of electrical contacts between two solid conductors. The problems of metal-to-metal and semiconductor-to-metal contacts are important technically, because they are directly related to electrical switches and rectifiers or detectors.

In 1930, Frenkel proposed that the anomalous temperature independence of contact resistance between metals could be explained in terms of tunneling across a narrow vacuum separation. Holm and Meissner (1932, 1933) then did careful measurements of contact resistances and showed that the magnitude and temperature independence of the resistance of insulating surface layers were in agreement with an explanation based on tunneling through a vacuumlike space. These measurements probably constitute the first correctly interpreted observations of tunneling currents in solids (Holm, 1967), since the vacuumlike space was a solid insulating oxide layer.

In 1932, Wilson, Frenkel, and Joffe, and Nordheim applied quantum mechanical tunneling to the interpretation of metal-semiconductor contacts–rectifiers such as those made from selenium or cuprous oxide. From a most simplified energy diagram, shown in Fig. 2, the following well known current–voltage relationship was derived:

$$J = J_s[\exp(eV/kT) - 1].$$

Apparently, this theory was accepted for a number of years until it was finally discarded after it was realized that it predicted rectification in the wrong direction for the ordinary practical diodes. It is now clear that, in the usual circumstances, the surface barriers found by the semiconductors in contact with metals, as illustrated in Fig. 2, are much too thick to observe tunneling current. There existed a general tendency in those early days of quantum mechanics to try to explain any unusual effects in terms of tunneling. In many cases, however, conclusive experimental evidence of tunneling was lacking, primarily because of the rudimentary stage of material science.

In 1934, the development of the energy-band theory of solids prompted Zener to propose interband tunneling, or internal field emission, as an explanation for dielectric breakdown. He calculated the rate of transitions from a filled band to a next-higher unfilled band by the application of an electric field. In effect, he showed that an energy gap could be treated in the manner of a potential barrier. This approach was refined by Houston in 1940. The Zener mechanism in dielectric breakdown, however, has never been proved to be important in reality. If a high electric field is applied to the bulk crystal of a dielectric or a semiconductor, avalanche breakdown (electron–hole pair generation) generally precedes tunneling, and thus the field never reaches a critical value for tunneling.

Around 1950, the technology of Ge p–n junction diodes, being basic to transistors, was developed, and efforts were made to understand the junction properties. In explaining the reverse-bias characteristic, McAfee *et al.* (1951) applied a modified Zener theory and asserted that low-voltage breakdown in Ge diodes (specifically,

$$J = AF^2 \exp(-4(2m)^{1/2}\phi^{3/2}/3\hbar F)$$
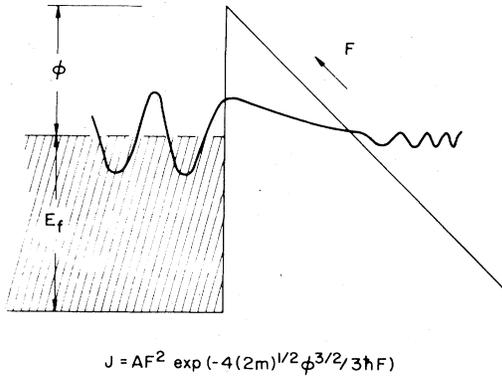
FIG. 1. Fowler–Nordheim tunneling.

they showed a 10 V breakdown) resulted from interband tunneling from the valence band in the p-type region to the empty conduction band in the n-type region. The work of McAfee *et al.* inspired a number of other investigations of breakdown in p–n junctions. Results of those later studies (McKay and McAfee, 1953; McKay, 1954; Miller, 1955) indicated that most Ge junctions broke down by avalanche, but by that time the name "Zener diodes" had already been given to the low-breaking Si diodes. Actually, these diodes are almost always avalanche diodes. In 1957, Chynoweth and McKay examined Si junctions of low-voltage breakdown and claimed that they had finally observed tunneling.

II. TUNNEL DIODE

In this circumstance, in 1956, I initiated the investigation of interband tunneling or internal field emission in semiconductor diodes primarily to scrutinize the electronic structure of narrow (width) p–n junctions. This information, at the time, was also important from a technological point of view.

The built-in field distribution in p–n junctions is determined by the profile of impurities—donors and acceptors. If both the impurity distributions are assumed to be

$$J = J_s\left(\exp\left(\frac{eV}{kT}\right) - 1\right)$$
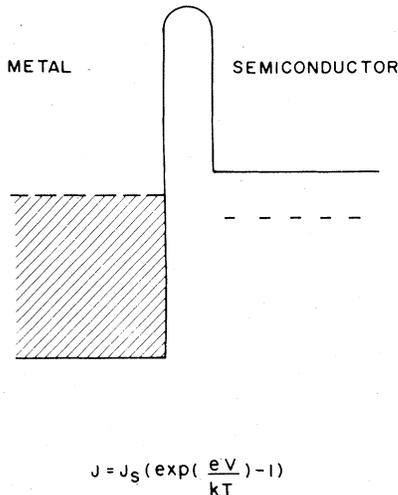
FIG. 2. Early model of metal-semiconductor rectifiers.

step functions, the junction width W is given by W = const $[(N_A + N_D)/N_A \cdot N_D]^{1/2} \sim 1/N^{1/2}$, where N_A and N_D are the acceptor and donor concentrations, and $N < N_A$ or N_D. Thus, first of all, we attempted to prepare heavily doped Ge p–n junctions. Both the donor and acceptor concentrations are sufficiently high so that the respective sides of the junctions are degenerate, that is, the Fermi energies are located well inside the conduction or valence band.

In this study, we first obtained a backward diode which was more conductive in the reverse direction than in the forward direction. In this respect it agreed with the rectification direction predicted by the previously mentioned old tunneling rectifier theory. The calculated junction width at zero bias was approximately 200 Å, which was confirmed by capacitance measurements. In this junction, the possibility of an avalanche was completely excluded because the breakdown occurs at much less than the threshold voltage for electron–hole pair production. The current-voltage characteristic at room temperature indicated not only that the major current-flow mechanism was convincingly tunneling in the reverse direction, but also that tunneling might be responsible for current flow even in the low-voltage range of the forward direction. When the unit was cooled, we saw, for the first time, a negative resistance, appearing, as shown in Fig. 3. By further narrowing the junction width (thereby further decreasing the tunneling path), through a further increase in the doping level, the negative resistance was clearly seen at all temperatures, as shown in Fig. 4 (Esaki, 1958).

The characteristic was analyzed in terms of interband tunneling. In the tunneling process, if it is elastic, the electron energy will be conserved. Figures (5(a), (b), (c),
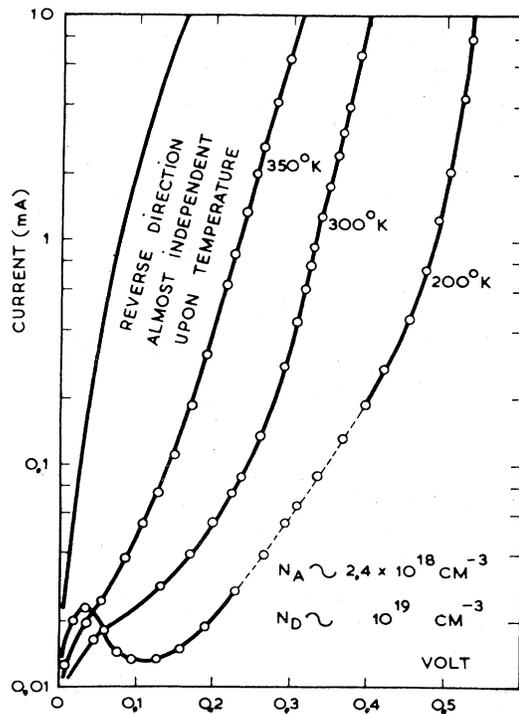
FIG. 3. Semilog plots of current–voltage characteristics in a tunnel diode, where $N_A \sim 2.4 \times 10^{18}$ cm^{-3}, and $N_D \sim 10^{19}$ cm^{-3}.
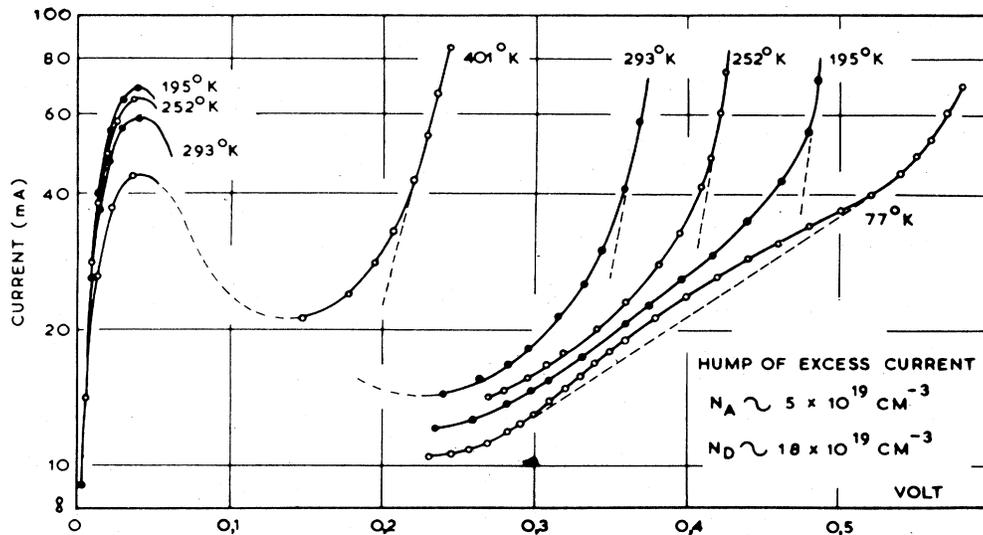
FIG. 4. Semilog plots of current–voltage characteristics in a tunnel diode, where $N_A \sim 5 \times 10^{19}$ cm^{-3}, and $N_D \sim 1.8 \times 10^{19}$ cm^{-3}.

and (d) show the energy diagrams of the tunnel diode at zero bias and with applied voltages, V_1, V_2, and V_3, respectively. As the bias is increased up to the voltage V_1, the interband tunnel current continues to increase, as shown by an arrow in Fig. 5(b). However, as the conduction band in the n-type side becomes uncrossed with the valence band in the p-type side, with further increase in applied voltages, as shown in Fig. 5(c), the current decreases because of the lack of allowed states of corresponding energies for tunneling. When the voltage reaches V_3 or higher, the normal diffusion (or thermal) current will dominate as in the case of the usual p–n diode. Semiconductor materials other than Ge were quickly explored to obtain tunnel diodes: Si, InSb, GaAs, InAs, PbTe, GaSb, SiC, etc.

In our early study of the Si tunnel diode (Esaki and Miyahara, 1960 and unpublished; Holonyak et al., 1959), a surprisingly fine structure was found in the current-

voltage curve at 4.2° K, indicating the existence of inelastic tunneling, as shown in Fig. 6. We were impressed with the fact that four voltages at the singularities shown in the figure agreed almost exactly with four characteristic energies due to acoustic and optical phonons, obtained from the optical absorption spectra (Macfarlane et al., 1959) and also derived from the analysis of intrinsic recombination radiation (Haynes et al., 1959) in pure silicon. The analysis of tunneling current in detail reveals not only the electronic states in the systems involved, but also the interactions of tunneling electrons with phonons, photons, plasmons, or even vibrational modes of molecular species in barriers.[1] As a result of the rich amount of information which can be obtained from a study of tunneling processes, a field called tunneling spectroscopy has emerged.

III. NEGATIVE RESISTANCE IN METAL-OXIDE-SEMICONDUCTOR JUNCTIONS

This talk, however, is not intended as a comprehensive review of the many theoretical and experimental investigations of tunneling, which is available elsewhere (Duke, 1969). Instead, I would like to focus on only one aspect for the rest of the talk; negative resistance phenomena in semiconductors which can be observed in novel tunnel structures.

Differential negative resistance occurs only in particular circumstances, where the total number of tunneling electrons transmitted across a barrier structure per second decreases, rather than increases as in the usual case, with an increase in applied voltage. The negative resistance phenomena themselves are not only important in solid state electronics because of possible signal amplification, but also shed light on some fundamental aspects of tunneling.

Before proceeding to the main subject, I would like to
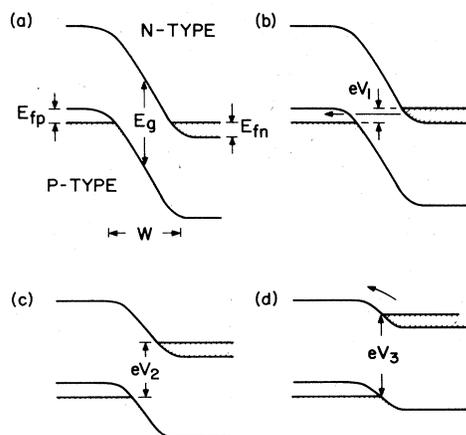
FIG. 5. Energy diagrams at varying bias conditions in the tunnel diode.

[1] See, for instance, Tunneling Phenomena in Solids 1969, edited by E. Burstein and S. Lundqvist (Plenum Press, New York).
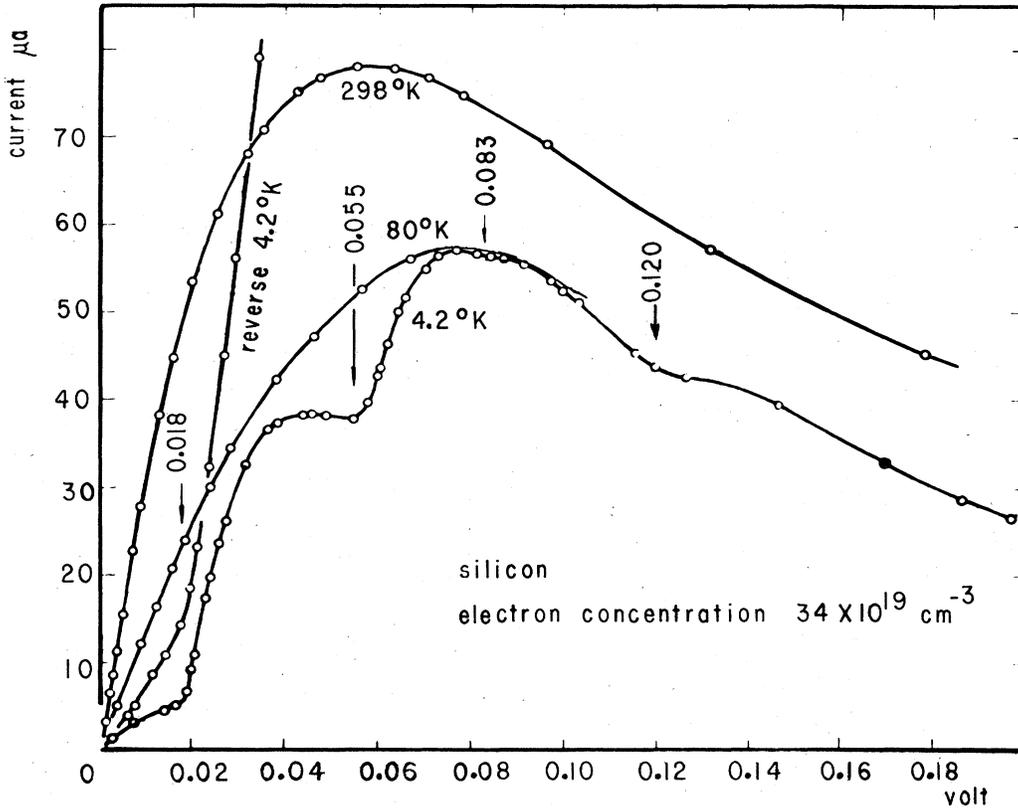
FIG. 6. Current–voltage characteristics in a Si tunnel diode at 4.2°, 80°, and 298°K.

briefly outline the independent-electron theory of tunneling (Harrison, 1961). In tunneling, we usually deal with a *one-dimensional potential barrier* $V(x)$. The transmission coefficient D for such a barrier is defined as the ratio of the intensity of the transmitted electron wave to that of the incident wave. The most common approximation for D is the use of the semiclassical WKB form

$$D(E_x) = \exp\left(-2/\hbar \int_{x_1}^{x_2} [2m(V - E_x)]^{1/2} dx\right), \quad (1)$$

where E_x is the kinetic energy in the direction normal to the barrier, and the quantities x_1 and x_2 are the classical turning points of an electron of energy E_x at the edges of the potential barrier. If the boundary regions are sharp, we first construct wave functions by matching values of functions as well as their derivatives at each boundary, then calculate the transmission coefficient D.

The tunneling expression should include two basic conservation laws: (1) Conservation of the total electron energy; and (2) Conservation of the component of the electron wave vector parallel to the plane of the junction. The velocity of an incident electron associated with a state of wave number k_x is given by $(1/\hbar)\partial E/\partial k_x$ in a one-particle approximation. Then, the tunneling current per second per unit area is written by

$$J = 2e/(2\pi)^3 \iiint D(E_x)$$

$$\times [f(E) - f(E')](1/\hbar)\partial E/\partial k_x dk_x dk_y dk_z, \quad (2)$$

where f is the Fermi distribution function or occupation

probability, and E and E' are the energy of the incident electron and that of the transmitted one, respectively. The front factor $2/(2\pi)^3$ comes from the fact that the volume of a state occupied by two electrons of the opposite spin is $(2\pi)^3$ in the wave-vector space for a unit volume crystal.

The previously mentioned tunnel diode is probably the first structure in which the negative resistance effect was observed. But, now, I will demonstrate that a similar characteristic can be obtained in a metal-oxide-semiconductor tunnel junction (Esaki and Stiles, 1966; Chang et al., 1967; Esaki, 1966), where the origin of the negative resistance is quite different from that in the tunnel diode. The semiconductors involved here (SnTe and GeTe) are rather unusual—more metallic than semiconducting; both of them are nonstoichiometric and highly p-type owing to high concentrations of Sn or Ge vacancies with typical carrier concentrations about 8×10^{20} and 2×10^{20} cm^{-3}, respectively. The tunnel junctions were prepared by evaporating SnTe or GeTe onto an oxidized evaporated stripe of Al on quartz or sapphire substrates. In contrast to the p–n junction diodes, all materials involved in these junctions are polycrystalline, although the Al oxide is possibly amorphous.

Figure 7 illustrates the current-voltage curves at 4.2° K of typical SnTe and GeTe junctions and Fig. 8 shows their energy diagrams at zero bias, and at applied voltages V_1 and V_2 from the left to the right. As is the case in the tunnel diode, until the bias voltage is increased such that the Fermi level in the metal side coincides with the top of the valence band in the semiconductor side [Fig.
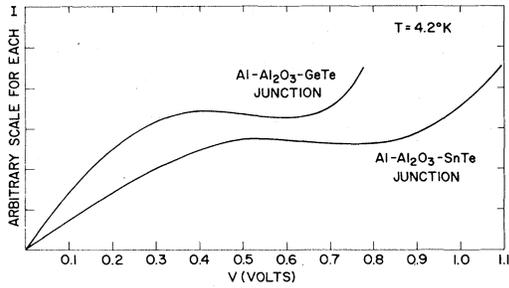
FIG. 7. Current–voltage characteristics in SnTe and GeTe tunnel junctions at 4.2°K.

FIG. 9. Energy diagrams at varying bias conditions in a double-barrier tunnel junction, indicating the resonant transmission in (b) and (d).

8(b)], the tunnel current continues to increase. When the bias voltage is further increased [Fig. 8(c)], however, the total number of empty allowed states or holes in the degenerate p-type semiconductor is unchanged, whereas the tunneling barrier height is raised, for instance from E_{BV_1} to E_{BV_2}, resulting in a decrease in tunneling probability and thus in current. As shown in Eq. (1), the tunneling probability is primarily determined by the exponential term, $\exp(-\lambda)$, where $\lambda \sim 2d(2mE_{BV})^{1/2}/\hbar$, and E_{BV} and d are the barrier height and width, respectively. Thus a negative resistance is exhibited in the current-voltage curve. When the bias voltage becomes higher than the level corresponding to the bottom of the conduction band in the semiconductor, a new tunneling path from the metal to the conduction band is opened and one sees the current again increasing with the voltage. The rectification direction in this junction is again backward, as is the case in the tunnel diode.

We might add that, in this treatment, the tunneling exponent is assumed to be determined only by the energy difference between the bottom of the conduction band in the oxide and the metal Fermi energy. This assumption should be valid because this energy difference is probably much smaller than that between the top of the valence band in the oxide and the metal Fermi energy.

IV. NEGATIVE RESISTANCE DUE TO RESONANT TRANSMISSION

It has been known that there is a phenomenon called the resonant transmission. Historically, resonant transmission was first demonstrated in the scattering of electrons by atoms of noble gases and is known as the

Ramsauer effect. In many textbooks[2] on quantum mechanics, the resonant transmission in tunneling or scattering is one of the more favored topics. In a one-dimensional double potential barrier (Kane, 1969), the narrow central potential well has weakly quantized (or quasistationary) bound states, of which the energies are denoted by E_1 and E_2 in Fig. 9(a). If the energy of incident electrons coincides with these energies, the electrons may tunnel through both barriers without any attenuation. As seen in Fig. 10 (two curves at $V = 0$), the transmission coefficient reaches unity at the electron energy $E = E_1$ or E_2. Since E_1 is a more strongly quantized state than E_2, the resonance peak at E_1 is much sharper than that at E_2. Although this sharpness depends upon the barrier thickness, one can achieve at some energy a resonance condition of 100% transmission, whatever thickness is given to the two barriers.

This effect is quite intriguing because the transmission

FIG. 8. Energy diagrams at varying bias conditions in Al–Al₂O₃–SnTe or –GeTe tunnel junctions.
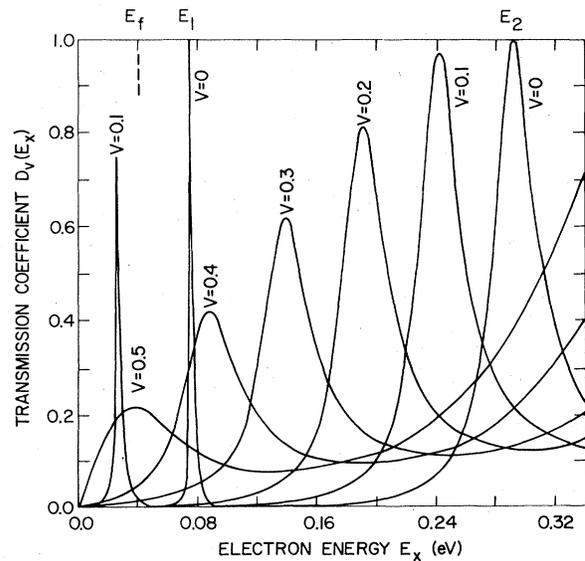
FIG. 10. Transmission coefficient versus electron energy, indicating the resonant transmission.

[2] See, for instance, D. Bohm, 1951, *Quantum Theory* (Prentice-Hall, New Jersey).

coefficient (or the attenuation factor) for two barriers is usually thought of as the product of two transmission coefficients, one for each barrier, resulting in a very small value for overall transmission. The situation, however, is somewhat analogous to the Fabry–Perot-type interference filer in optics. The high transmissivity arises because, for certain wavelengths, the reflected waves from inside interfere destructively with the incident waves, so that only a transmitted wave remains.

This resonating condition can be extended to a periodic barrier structure. In the Kronig–Penney model of a one-dimensional crystal which consists of a series of equally spaced potential barriers, it is well known that allowed bands of perfect transmission are separated by forbidden bands of attenuation. These one-dimensional mathematical problems can often be elegantly treated, leading to exact analytical solutions in textbooks of quantum mechanics. Many of these problems, however, are considered to be pure mathematical fantasy, far from reality.

We recently initiated an experimental project to materialize one-dimensional potential barriers in monocrystalline semiconductors in order to observe the predicted quantum-mechanical effects (Esaki and Tsu, 1970; Esaki et al., 1972). We choose n-type GaAs as a host semiconductor or a matrix in which potential barriers with the height of a fraction of one electron volt are made by inserting thin layers of $Ga_{1-x}Al_xAs$ or AlAs. Because of the similar properties of the chemical bond of Ga and Al together with their almost equal ion size, the introduction of AlAs into GaAs makes the least disturbance to the quality of single crystals. And yet the difference in the electronic structure between the two materials makes a sharp potential barrier inside the host semiconductor. We prepare the multilayer structure with the technique of molecular beam epitaxy in ultrahigh vacuum environment. Precise control of thickness and composition has been achieved by using a process control computer (Chang et al., 1973).

With this facility, a double potential barrier structure has been prepared (Chang et al., to be published), in which the barrier height and width are about 0.4 eV and a few tens of angstroms, respectively, and the width of the central well is as narrow as 40–50 Å. From these data,
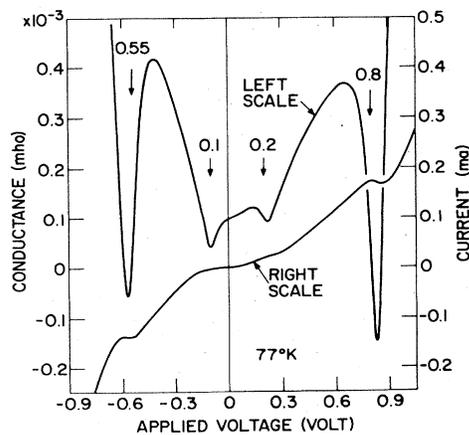
the first two energies, E_1 and E_2, of the weakly quantized states in the well are estimated to be 0.08 and 0.30 eV.

We have measured the current–voltage characteristic as well as the conductance dI/dV as a function of applied voltages in this double tunnel junction. The results at 77° K are shown in Fig. 11, and they clearly indicate two singularities in each polarity and even show a negative resistance around + 0.8 volt or -0.55 volt. The applied voltages at the singularities, averaged in both polarities, are roughly twice as much as the calculated bound-state energies. This general feature is not much different at 4.5° K, although no structure is seen at room temperature.

The energy diagrams at zero bias and at applied voltages V_1, V_2 and V_3 are shown in Fig. 9. The electron densities on both the left and right GaAs sides are about 10^{18} cm^{-3} which gives a Fermi energy of 0.04 eV at zero temperature. These electrons are considered to be classical free carriers with the effective mass, m^*, of which the kinetic energy E is given by

$$E = (\hbar^2/2m^*)(k_x^2 + k_y^2 + k_z^2).$$

On the other hand, the electrons in the central well have the weakly quantized levels, E_1, E_2, ..., for motion in the x direction perpendicular to the walls with a continuum for motion in the y–z plane parallel to the walls. These electrons are nearly two-dimensional, which is to say the kinetic energy E is given by

$$E = E_i + (\bar{n}^2/2m^*)(k_y^2 + k_z^2).$$

An approximation is made that the same electron effective mass, m^*, exists throughout the structure. Then an expression for the tunneling current in this structure (Tsu and Esaki, 1973) can be derived in the framework of the previously described tunneling formalism in Eq. (2). Using $\partial E/\partial k_x = \partial E_x/\partial k_x$, $2\pi k_t dk_t = dk_y dk_z$, and T (temperature) = 0, the current is given by

$$J = e/2\pi^2\hbar \int_0^{E_f} D(E_x) \int_0^{[2m^*(E_f-E_x)]^{1/2}/\hbar} k_t dk_t dE_x$$
$$- e/2\pi^2\hbar \int_0^{E_f-eV} D(E_x) \int_0^{[2m^*(E_f-E_x-eV)]^{1/2}/\hbar} k_t dk_t dE_x, \quad (3)$$

where V is the applied voltage, on which the transmission coefficient $D(E_x)$ depends. The above expression can be integrated over the transverse wave number k_t, giving

$$J = em^*/2\pi^2\hbar^3 \int_0^{E_f} D_V(E_x)(E_f - E_x)dE_x$$
$$- em^*/2\pi^2\hbar^3 \int_0^{E_f-eV} D_V(E_x)(E_f - E_x - eV)dE_x. \quad (4)$$

In both Eqs. (3) and (4), the second term is nonzero only for $eV < E_f = 0.04$ eV.

Now, the transmission coefficient $D_V(E_x)$ can be derived for each applied voltage from wave functions which are constructed by matching their values as well as derivatives at each boundary. Figure 10 shows one example of calculated D as a function of the electron energy for applied voltages between zero and 0.5 volt. The energy zero is taken at the bottom of the conduction band on the left as shown in Fig. 9. In this example, the well width is taken to be 45 Å and the barrier height 0.4 eV at zero bias. The square shape for barriers and well is assumed for simplicity of calculation, although they are

FIG. 11. Current, I, and conductance, dI/dV, versus voltage curves in a double barrier tunnel junction.

TWO-DIMENSIONAL
ELECTRON GAS
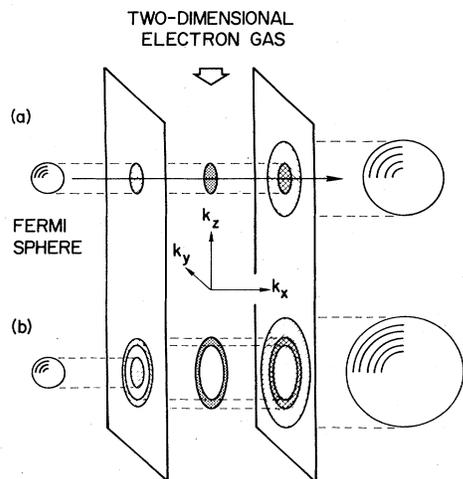
FIG. 12. Construction of shadows of energy surfaces on two k_y-k_z planes corresponding to two barriers.

actually trapezoidal at any applied voltage.

Referring to Figs. 9 and 10, both the absolute values and the positions in energy for the maxima of the transmission coefficient decrease with increasing applied voltages, the origin of energy being the conduction band edge for the left outer GaAs layer. The current maxima occur at applied voltages such that the electron energies on the left coincide with the bound-state energies, as illustrated in Figs. 9(b) and 9(d). This resonant transmission has been experimentally verified as shown in Fig 11. The transmission coefficient itself at this resonance, however, is appreciably less than unity as indicated in Fig. 10, primarily because of the asymmetric nature of the potential profile at applied voltages.

To gain an insight into this tunneling problem, particularly in view of the transverse wave-vector conservation (specular tunneling), a representation in the wave-vector space is useful and is shown in Fig. 12. Two $k_y - k_z$ planes are shown parallel to the junction plane, corresponding to the two barriers. Figures 12(a) and 12(b) show two different bias-voltage conditions. First, the Fermi sphere on the left is projected on the first screen, making a circle. A similar projection, of the two-dimensional electrons in the central well which have the same total energies as electrons in the Fermi sphere on the left at the particular applied voltage, will form a circle [Fig. 12(a)], or a ring [Fig. 12(b)], depending upon the value of applied voltage. If the two projected patterns have no overlap, there will be no specular tunneling current. The situation on the right screen is slightly different, since an energy sphere on the right, in which electrons have the same total energies as electrons in the Fermi sphere on the left, is rather large; moreover, its size will be increased as the applied voltage increases. Thus in this case the two projected patterns always overlap. Figures 12(a) and 12(b) correspond to the bias conditions in Figs. 9(b) and 9(c), respectively. With an increase in applied voltage from V_1 to V_2, the current will decrease because of a disappearance of overlapping regions, thereby causing a negative resistance. Since the current density is dependent upon the half-width of the resonant peaks shown in Fig. 10, we have observed a clear negative resistance
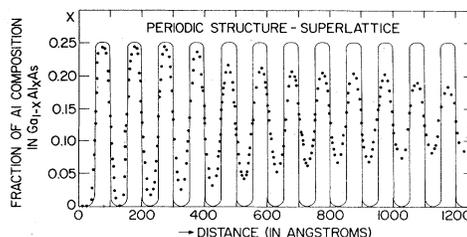
FIG. 13. Composition profile of a superlattice structure measured by a combination of ion sputter-etching and Auger electron spectroscopy.

associated with the second bound-state which is not swamped by possible excess currents arising for a variety of reasons.

V. PERIODIC STRUCTURE SUPERLATTICE

The natural extension of double barriers will be to construct a series of tunnel junctions by a periodic variation of alloy composition (Esaki and Tsu, 1970; Esaki et al., 1972). By using the same facilities for computer-controlled molecular beam epitaxy, we tried to prepare a Kronig–Penney-type one-dimensional periodic structure—a man-made superlattice with a period of 100 Å (Chang et al., 1973). The materials used here are again GaAs and AlAs or $Ga_{1-x}Al_x$As.

The composition profile of such a structure (Ludeke et al., unpublished) has been verified by the simultaneous use of ion sputter-etching of the specimen surface and Auger electron spectroscopy, and is shown in Fig. 13. The amplitudes of the Al Auger signals serve as a measure of Al concentration near the surface within a sampling depth of only 10 Å or so. The damping of the oscillatory behavior evident in the experimental data is not due to thermal diffusion or other reasons but due to a surface-roughening effect or nonuniformity in the sputter-etching process. The actual profile, therefore, is believed to be the one which is illustrated by the solid line in Fig. 13. This is certainly one of the highest resolution structures ever built in monocrystalline semiconductors.

It should be recognized that the period of this superlattice is ~ 100 Å—still large in comparison with the crystal lattice constant. If this period l, however, is still shorter than the electron mean free path, a series of narrow
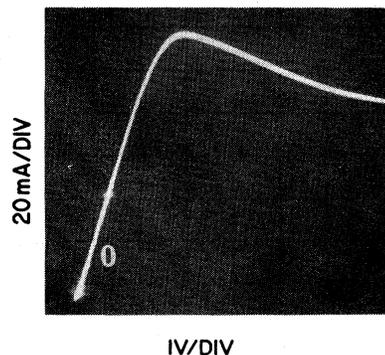
IV/DIV

FIG. 14. Current–voltage characteristic at room temperature of a 70 Å period, $GaAs$–$Ga_{0.5}Al_{0.5}As$ superlattice.

allowed and forbidden bands is expected, because of the subdivision of the original Brillouin zone into a series of minizones. If the electron scattering time τ, and an applied electric field F, meet a threshold condition: $eF\tau l/\hbar > 1$, the combined effect of the narrow energy band and the narrow wave-vector zone makes it possible for electrons to be excited beyond an inflection point in the energy-wave vector relation. This would result in a negative resistance for electrical transport in the direction of the superlattice. This can be seen in another way. The de Broglie wavelength of conduction electrons having an energy of, for instance, 0.03 eV in n-type GaAs (the effective mass $\sim 0.1m$), is of the order of 200 Å. Therefore, an interaction of these electron waves with the Kronig–Penney-type potential with a period of 100 Å can be expected, and will give rise to a nonlinear transport property.

We have begun to observe such current–voltage characteristics as shown in Fig. 14. The observed negative resistance may be interesting not only from the scientific aspect but also from a practical viewpoint because one can expect, at least theoretically, that the upper limit of operating frequencies would be higher than that for any known semiconductor devices.

VI. CONCLUSION

I am, of course, deeply aware of important contributions made by many colleagues and my friends throughout this long journey. The subject of Sec. II was carried out when I was in Japan, and all the rest[3] has been performed in the United States of America. Since my journey into tunneling is still continuing, I do not come to any conclusions in this talk. However, I would like to point out that many high barriers exist in this world: Barriers between nations, races and creeds. Unfortunately, some barriers are thick and strong. But I hope, with determination, we will find a way to tunnel through these barriers easily and freely, to bring the world together so that everyone can share in the legacy of Alfred Nobel.

REFERENCES

Bohm, D., 1951, *Quantum Theory* (Prentice-Hall, New Jersey).
Burstein, E., and S. Lundqvist, 1969, Eds., *Tunneling Phenomena in Solids* (Plenum Press, New York).

Chang, L. L., P. J. Stiles, and L. Esaki, 1967, J. Appl. Phys. **38**, 4440.
Chang, L. L., L. Esaki, W. E. Howard, and R. Ludeke, 1973, J. Vac. Sci. Technol. **10**, 11.
Chang, L. L., L. Esaki, W. E. Howard, R. Ludeke, and G. Schul, 1973, J. Vac. Sci. Technol. **10**, 655.
Chang, L. L., L. Esaki, and R. Tsu, to be published.
Chynoweth, A. G., and K. G. McKay, 1957, Phys. Rev. **106**, 418.
de Broglie, L., 1923, Nature (Lond.) **112**, 540.
de Broglie, L., 1925 , Ann. Phys. (Paris), 10 Ser. **3**, 22.
Duke, C. B., 1969 *Tunneling in Solids* (Academic, New York).
Esaki, L., 1958, Phys. Rev. **109**, 603.
Esaki, L., 1960, "Solid State Physics in Electronics and Telecommunications," in Proceedings of the International Conference Sponsored by the Postal and Telecommunications Group of the Brussels Universal Exhibition, Brussels, 1958, edited by M. Desirant and J. L. Michels (Academic, New York), Vol. 1, *Semiconductors*, Part I, p. 514.
Esaki, L., 1966, J. Phys. Soc. Jap. Suppl. **21**, 589.
Esaki, L., and Y. Miyahara, 1960, Solid-State Electron. **1**, 13.
Esaki, L., and Y. Miyahara, unpublished.
Esaki, L., and P. J. Stiles, 1966, Phys. Rev. Lett. **16**, 1108.
Esaki, L., and R. Tsu, 1970, IBM J. Res. Dev. **14**, 61.
Esaki, L., L. L. Chang, W. E. Howard, and V. L. Rideout, 1972, in *Proceedings of the 11th International Conference on the Physics of Semiconductors*, Warsaw, Poland, 1972, p. 431.
Fowler, R. H., and L. Nordheim, 1928, Proc. R. Soc. Lond. A **119**, 173.
Frenkel, J., 1930, Phys. Rev. **36**, 1604.
Frenkel, J., and A. Joffe, 1932, Phys. Z Sowjetunion **1**, 60.
Gamow, G., 1928, Z. Phys. **51**, 204.
Gurney, R. W., and E. U. Condon, 1928, Nature (Lond.) **122**, 439.
Harrison, W. A., 1961, Phys. Rev. **123**, 85.
Haynes, J. R., M. Lax, and W. F. Flood, 1959, J. Phys. Chem. Solids **8**, 392.
Holm, R., 1967, *Electric Contacts* (Springer-Verlag, New York), p. 118.
Holm, R., and W. Meissner, 1932, Z. Phys. **74**, 715.
Holm, R., and W. Meissner, 1933, Z. Phys. **86**, 787.
Holonyak, K. B., I. A. Lesk, R. N. Hall, J. J. Tiemann, and H. Ehrenreich, 1959, Phys. Rev. Lett. **3**, 167.
Houston, W. V., 1940, Phys. Rev. **57**, 184.
Kane, E. O., 1969, in *Tunneling Phenomena in Solids*, edited by E. Burstein and S. Lundqvist (Plenum, New York), pp. 9–11.
Lilienfeld, J. E., 1922, Phys. Z. **23**, 506.
Ludeke, R., L. Esaki, and L. L. Chang, to be published.
Macfarlane, G. G., T. P. McLean, J. E. Quarrington, and V. Roberts, 1959, J. Phys. Chem. Solids **8**, 388.
McAfee, K. B., E. J. Ryder, W. Shockley, and M. Sparks, 1951, Phys. Rev. **83**, 650.
McKay, K. G., 1954, Phys. Rev. **94**, 877.
McKay, K. G., and K. B. McAfee, 1953, Phys. Rev. **91**, 1079.
Miller, S. L., 1955, Phys. Rev. **99**, 1234.
Nordheim, L., 1932, Z. Phys. **75**, 434.
Oppenheimer, J. R., 1928a, Phys. Rev. **31**, 66.
Oppenheimer, J. R., 1928b, in Proc. Natl. Acad. Sci. USA **14**, 363.
Rice, O. K., 1929, Phys. Rev. **34**, 1451.
Schrödinger, E., 1926, Ann. Phys. (Leipz.), 4 Folge **79**, 361, 489.
Tsu, R., and L. Esaki, 1973, Appl. Phys. Lett. **22**, 562.
Wilson, A. H., 1932, Proc. R. Soc. Lond. A **136**, 487.
Zener, C., 1934, Proc. R. Soc. Lond. **145**, 523.

FIG. 14. Current–voltage characteristic at room temperature of a 70 Å period, GaAs–Ga$_{0.5}$Al$_{0.5}$As superlattice.